Materials Horizons

COMMUNICATION

View Article Online
View Journal | View Issue

Cite this: *Mater. Horiz.*, 2017, 4, 1102

Received 22nd May 2017,
Accepted 21st August 2017

DOI: 10.1039/c7mh00345e

rsc.li/materials-horizons

Organic liquid-crystal devices based on ionic conductors†

Can Hui Yang,[abc] Shuang Zhou,[ac] Samuel Shian,[a] David R. Clarke[a] and Zhigang Suo*[ac]

A fully organic liquid-crystal device is enabled by ionic conductors. The device uses a liquid crystal as a voltage-driven light shutter, an elastomer as a transparent dielectric, and a hydrogel as a transparent conductor. A voltage switches the device from an opaque state to a transparent state without electrolyzing the hydrogel. The device maintains its electrooptical performance under a biaxial stretch of 1.5.

Conceptual insights

Conventional liquid-crystal devices are stiff and brittle, struggling to satisfy the fast growing demands for mobile and wearable applications. Here we demonstrate fully organic liquid-crystal devices (OLCDs) based on ionic conductors. A liquid crystal is encapsulated in a dielectric elastomer cell, and then sandwiched between ionic conducting gels. The OLCDs achieve the same electrooptical characteristics as the liquid-crystal devices using electronic conductors. The OLCDs maintain their electrooptical performance under biaxial stretching. The OLCDs are amenable to roll-to-roll and digital manufacturing. The softness of the devices may bring liquid crystals to new domains of applications, such as wearable displays for camouflage and entertainment. One can also imagine programmable, high-resolution, and tissue-attachable patterns of light for optogenetics and optoceuticals—that is, a direct TV for the brain, heart, and skin.

Liquid crystals have enabled many electrooptical devices, including liquid-crystal displays,[1] universal optical phase modulators,[2] beam steering devices,[3] tunable Fresnel lenses,[4,5] broad-spectrum tunable color reflectors, and nanosecond light modulators.[6,7] These devices require transparent conductors to apply voltage and let light pass through. The widely used transparent conductor, indium tin oxide (ITO), is a brittle and costly inorganic material, and requires a vacuum for deposition. Great efforts have been devoted to the development of new transparent conductors, usually using soft matrices to host conducting materials, such as conducting polymers,[8–10] carbon nanotubes,[11–13] graphene,[14–16] nanoparticulate metal oxides,[17] and silver nanowires.[18–20]

These conductors, like ITO, carry electricity using electrons. The development of transparent electronic conductors has many challenges. First, conducting electrons reflect or absorb light, so electronic conductors cannot simultaneously achieve high electrical conductance and high optical transmittance. Second, most electronic conductors are hard inorganic materials, prone to fracture and delamination under monotonic and cyclic stretching.[21–23] Patterning or pre-straining can make composite electrodes stretchable, but constituent materials remain mechanically mismatched.[24–28] Third, devices requiring materials of very different processing conditions may cause additional technical issues for roll-to-roll fabrication and digital manufacturing.[29,30] These challenges limit further development of electronic conductors for flexible and wearable devices, especially when large stretchability becomes essential.

Here we show that liquid-crystal devices can operate without electronic conductors, but with ionic conductors. We use polymer gels as transparent ionic conductors to realize fully organic liquid-crystal devices (OLCDs). They achieve the same electrooptical characteristics as liquid crystal devices using electronic conductors. The OLCDs perform electrooptical functions without electrochemical reactions. Furthermore, the polymer gels are stretchable, so that the OLCDs are optically responsive to both mechanical force and electrical voltage; they are mechanooptical and electrooptical devices.

Many polymer gels are stretchable, transparent, and ionic conductors.[31] For example, a hydrogel is a polymer network swollen with water, and can dissolve ions of multiple moles per liter, leading to a resistivity of $\sim 10^{-1}$ Ω m.[32] Even through this resistivity is much higher than that of ITO ($\sim 10^{-5}$ Ω m), a millimeter-thick hydrogel can achieve a surface resistance of 100 Ω and retain an optical transparency of 99.9%.[31] The softness

[a] *John A. Paulson, School of Engineering and Applied Science, Harvard University, Cambridge, MA 02138, USA. E-mail: suo@seas.harvard.edu*
[b] *International Center for Applied Mechanics, State Key Laboratory for Strength and Vibration of Mechanical Structures, School of Aerospace, Xi'an Jiaotong University, Xi'an, 710049, China*
[c] *Kavli Institute for Bionano Science and Technology, Harvard University, Cambridge, MA 02138, USA*

† Electronic supplementary information (ESI) available. See DOI: 10.1039/c7mh00345e

of the gels allows large and elastic deformation over many cycles.[31,33–37] The properties of hydrogels can be tuned by adjusting the cross-linkers.[38–40] Hydrogels as tough as natural rubber have been demonstrated.[41,42] Hydrogels can retain water in a low-humidity environment if they contain humectants,[32] or are encapsulated in low-permeability elastomers.[43,44] As another example, an ionogel is a polymer network swollen with an ionic liquid. Ionogels are nonvolatile even under vacuum,[35] and can access a wide range of temperatures through suitable choices of ionic liquid.[45] In addition, a nanostructured organic liquid crystal polymer electrolyte also achieves ionic conductivity on the order of 10 Ω m.[46]

Recent works have demonstrated that ionic conductors can enable devices of unusual characteristics. Devices of high voltage (10 kV)[31,35] and high frequency (up to 100 MHz)[47] have been demonstrated, as well as artificial muscles, axons, and skin.[31,47–49] Potential applications include transparent loudspeakers and active noise cancelation,[31] strain and pressure sensors,[43,50–52] and stretchable touch pads.[53] The soft devices can be made attachable to living tissues and soft robots. Ionic conductors have also enabled ionotronic devices, which integrate ionic conductors and electronic conductors. Examples include the rocking-chair operation of light-emitting diodes[47] and stretchable electroluminescence.[48,49,54]

We now introduce ionic conductors in liquid-crystal devices. Although the principle applies to all liquid-crystal devices, here as a proof of concept we demonstrated a voltage-driven light shutter (Fig. 1). A cholesteric liquid crystal is encapsulated in a dielectric cell, sandwiched between ionic conductors, and connected *via* electronic conductors to an external voltage source. We do not treat the surfaces of the dielectric cell with mechanical rubbing or alignment agents, so that the liquid-crystal molecules orient randomly on the dielectric surfaces. When voltage is off, the cholesteric forms a focal conic texture (twist domains with a randomly orientated helical axis), the domain boundaries scatter light, and the device is opaque (Fig. 1a). When voltage is on, the electric field unwinds the twisted domains, the liquid-crystal molecules align into a homeotropic state and the device is transparent (Fig. 1b). The dielectric cell is made of an elastomer, and the ionic conductors are made up of gels; they are transparent and stretchable. The electronic conductors are opaque and rigid metal foils; they contact the ionic conductors outside the area of the liquid crystals, and do not affect the transmittance and stretchability of the device.

Each interface between an ionic conductor and an electronic conductor forms an electric double layer (EDL). As shown below, the voltage drop over each EDL is much lower than 1 V, so that the EDL remains stable, and behaves like a capacitor, C_{EDL}, in series with capacitors due to the dielectric elastomers and the liquid crystals, C_D and C_{LC}, as well as the resistors due to the ionic conductors, R_{gel} (Fig. 1c).

We use three layers of an acrylic elastomer (VHB 4905, 3M) to make a dielectric cell, two layers of a polyacrylamide hydrogel

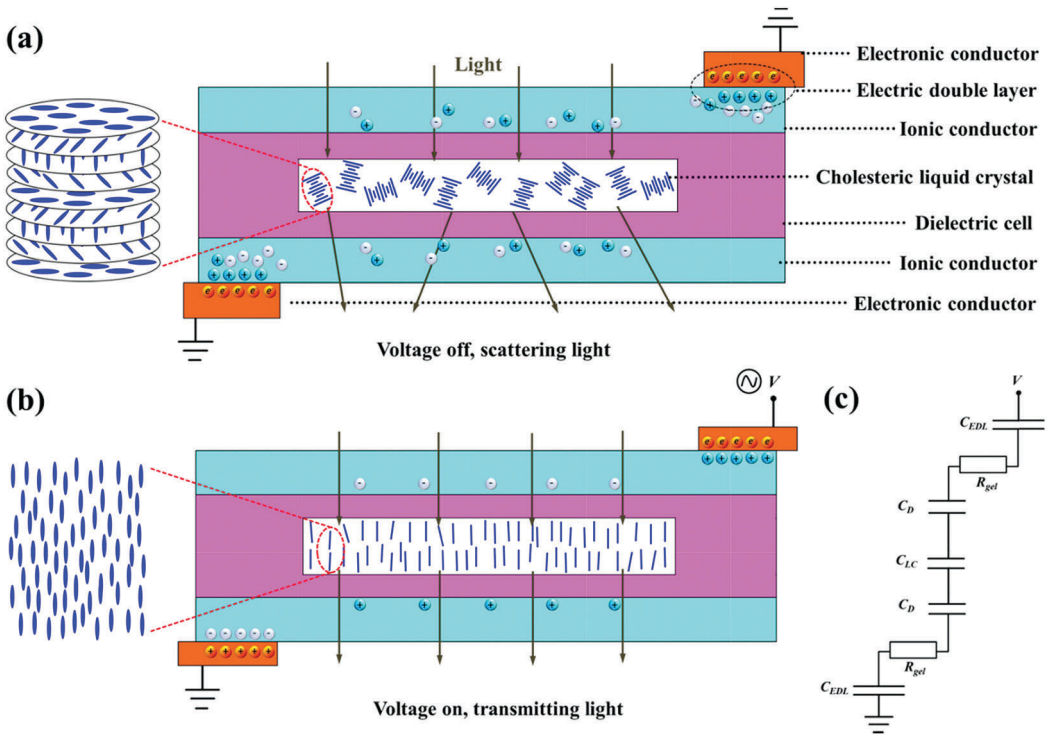

Fig. 1 Organic liquid-crystal device based on ionic conductors. (a) A cholesteric liquid crystal is encapsulated in a dielectric cell, sandwiched between ionic conductors, and connected *via* electronic conductors to an external voltage source. When the external voltage is off, the liquid crystal molecules form twisted domains, the domain boundaries scatter light, and the device is opaque. (b) When the external voltage is on, the domains unwind, the molecules align with the electric field, and the device is clear. (c) Equivalent circuit of the device.

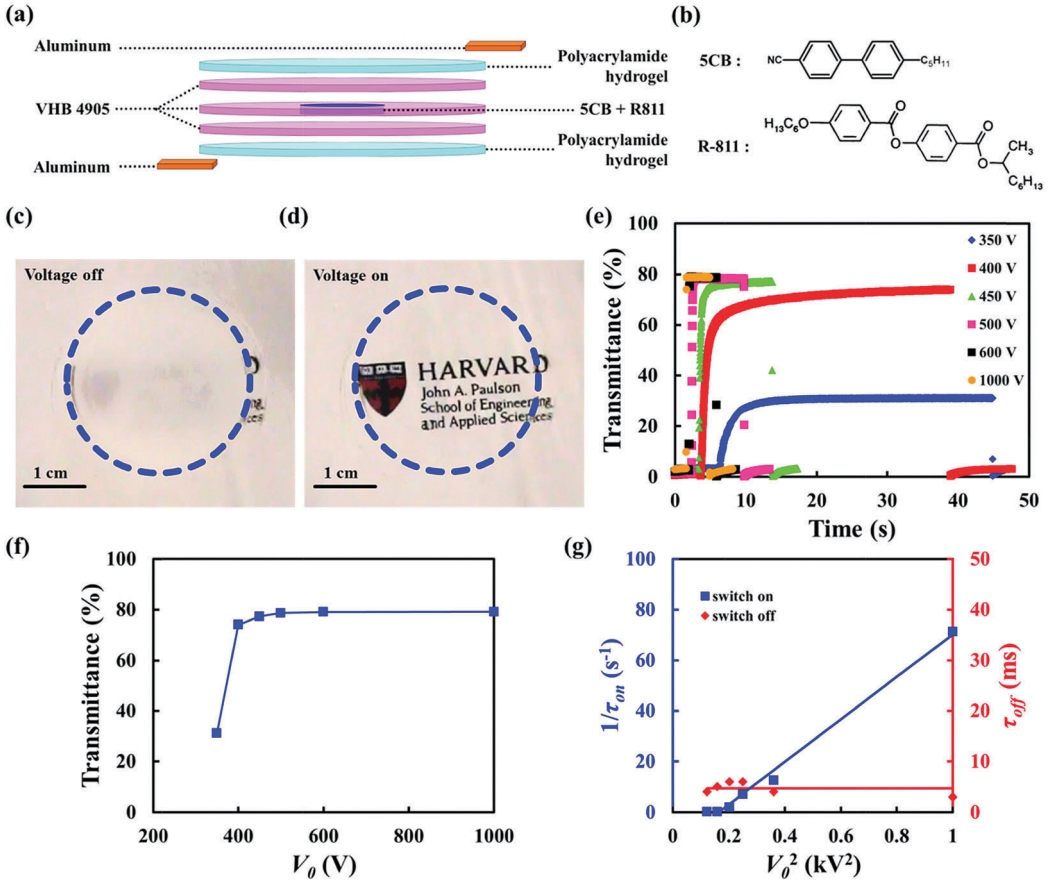

Fig. 2 Electrooptical characteristics. (a) Schematic of a liquid-crystal device. (b) Molecular structures of the nematic liquid crystal 5CB and the chiral dopant R-811. (c) When voltage is off, the device is opaque. (d) When voltage is on, the device is transparent. A square-wave voltage is applied at an amplitude of 600 V and a frequency of 1 kHz. The dashed circles indicate the areas containing the liquid crystal. (e) Transmittance of the device as a function of time at square-wave voltages of various amplitudes at a frequency of 1 kHz. (f) The transmittance of the device increases and then saturates as voltage increases. (g) $1/\tau_{on}$ increases linearly with the voltage square, and τ_{off} is almost constant. The solid lines are linear-fitting curves.

containing 8.0 M lithium chloride as the ionic conductor, and two pieces of aluminum as the electronic conductors (Fig. 2a). We form the cholesteric liquid crystal by mixing a nematic (5CB, 95.0 wt%) and a chiral dopant (R-811, 5.0 wt%) (Fig. 2b). The cholesteric has the same thickness as the middle layer of the dielectric cell. When voltage is off, the area covered by the cholesteric is opaque, and the area covered by the hydrogel and elastomer is transparent (Fig. 2c). When voltage is on, the cholesteric becomes transparent (Fig. 2d). We apply an alternating voltage to prevent space charges from accumulating at the interfaces between the cholesteric and the dielectric. Such space charges would build an internal electric field to counteract the applied electric field.[1]

After the voltage is switched on, the transmittance of the device increases with time and then saturates (Fig. 2e and Movie S1, ESI†). The saturated transmittance increases as the voltage increases, and plateaus at large voltages (Fig. 2f). We measure the switch-on time τ_{on} and switch-off time τ_{off} (Fig. S1, ESI†).[1] The inverse of the measured switch-on time is proportional to the square of the voltage, $\frac{1}{\tau_{on}} \propto V_0^2$, and the switch-off time is nearly independent of voltage (Fig. 2g).

We next relate the observed electrooptical characteristics to fundamental principles. The applied voltage should be low enough to avert the electrical breakdown in the cholesteric and the dielectric, and avert the electrolysis of the gel. We estimate the voltage drop on each component by comparing their impedances. The resistance of the hydrogel is $R_{gel} \sim 10^2\ \Omega$, given that the thickness is $\sim$1 mm, length is $\sim$1 cm and width is $\sim$1 cm, and resistivity is $\sim 10^{-1}\ \Omega$ m. The capacitance per unit area of the EDL is $c_{EDL} \approx 10^{-1}$ F m^{-2},[55] the area of the EDL is $A_{EDL} \approx 10^{-4}$ m^2, and the angular frequency is $\omega = 2\pi f = 2000\pi$, so that the impedance of the EDL is $|Z_{EDL}| = \frac{1}{\omega c_{EDL} A_{EDL}} \approx 15\ \Omega$. The capacitance of the dielectric (VHB) is $C_D = \varepsilon_{VHB}\varepsilon_0 A_{active}/d_{VHB} \approx 2.1 \times 10^{-9}$ F, where $\varepsilon_{VHB} \approx 4.7$ is the dielectric constant of VHB,[56] $\varepsilon_0 = 8.85 \times 10^{-12}$ F m^{-1} is the permittivity of vacuum, $d_{VHB} \sim 20$ μm is the thickness of VHB 4905 under a biaxial pre-stretch of $\sim$5, and $A_{active} \sim 10^{-3}$ m^2 is the area of the active region containing the cholesteric, so that the impedance of the dielectric is $|Z_D| = \frac{1}{\omega C_D} \approx 7.65 \times 10^4\ \Omega$. The cholesteric has the same thickness and area as the VHB layer. The orientations of the liquid-crystal molecules

are random in the voltage off state and the isotropic (or average) dielectric constant of 5CB is $\varepsilon_{5CB}^{iso} \approx 11$; we use $\varepsilon_{5CB}^{\parallel} \approx 20$, the dielectric constant parallel to the director, for estimation,[57] since the equilibrium state has liquid-crystal molecules parallel to the field. We estimate that $C_{CLC} \approx 8.85 \times 10^{-9}$ F and $|Z_{CLC}| = \frac{1}{\omega C_{CLC}} \approx 1.8 \times 10^4\ \Omega$. For the applied voltage of 600 V, the voltage drop across the EDL is ~52.5 mV, which is much lower than the threshold voltage for the electrolysis of water. The voltage drop on the hydrogel is ~350.4 mV. The main voltage drops are on the cholesteric, ~63.1 V, and on the dielectrics, ~268.1 V, for each VHB layer. The electric field in the dielectric is ~13.4 MV m^{-1}, which is much smaller than the electrical breakdown field of VHB (~100 MV m^{-1}).[51] Similarly, the electric field in the cholesteric is below the electrical breakdown field of the cholesteric (~10 MV m^{-1}).[58,59]

The applied voltage should be high enough to switch the liquid-crystal molecules from the twisted domains to the homeotropic state. The threshold electric field is given by $E_{th} = \frac{\pi^2}{p}\sqrt{\frac{K_2}{\Delta\varepsilon\varepsilon_0}}$.[57] For the 5CB/R-811 mixture, the twist elastic constant is $K_2 = 3 \times 10^{-12}$ N, the dielectric anisotropy is $\Delta\varepsilon = 13$, and the pitch is determined as $p = \frac{1}{HTP \cdot c} \approx 2\,\mu m$, where the HTP of ~10 μm^{-1} is the helical twisting power of R-811 in 5CB, and c = 5.0 wt% is the concentration of R-811.[1] Consequently, the threshold electric field to unwind the cholesteric is $E_{th} \sim$ 0.8 MV m^{-1}. This estimate is consistent with our observation that the device becomes transparent at 350 V, which gives $E \sim 1.84$ MV m^{-1} in the cholesteric (Fig. 2d).

Similar to the dynamic process of the Fredericks transition in liquid crystals,[60,61] the switch-on time τ_{on} scales as $\frac{1}{\tau_{on}} \propto \frac{1}{\eta_{twist}}\left|\Delta\varepsilon\varepsilon_0 E^2 - \left(\frac{2\pi}{p}\right)^2 K_2\right|$, where η_{twist} is the rotational viscosity of the liquid crystal. The large electric field E shortens the switch-on time. For the cholesteric of rotational viscosity $\eta_{twist} \sim 80$ mPa s,[1] the theoretical limit of switch-on time can reach the order of 10^{-5} s when the electric field is just below the electrical breakdown field of the liquid crystal of 10 MV m^{-1}. The switch-on time in our experiment reaches ~14 ms when the voltage is 1000 V. A faster response can be achieved under a higher voltage theoretically; however, our experiment is limited by the timing loop of the data acquisition program.

Switching off is a field-independent process of several stages. When the voltage is switched off, the liquid-crystal molecules transit from the homeotropic state to the planar state, and then from the planar state to the focal conic state. The dynamics of the nucleation process depends on the impurities in the cholesteric and irregularities on the dielectric surface. As expected, the measured switch-off time is a constant independent of the voltage applied (Fig. 2f). For comparison, we fabricate a device by using ITO glass as the electrode and VHB with a similar thickness (~20 μm) as the spacer. The switch-off time remains constant, ~8.2 ms, at various applied voltages (Fig. S2, ESI†). The liquid-crystal devices using ionic

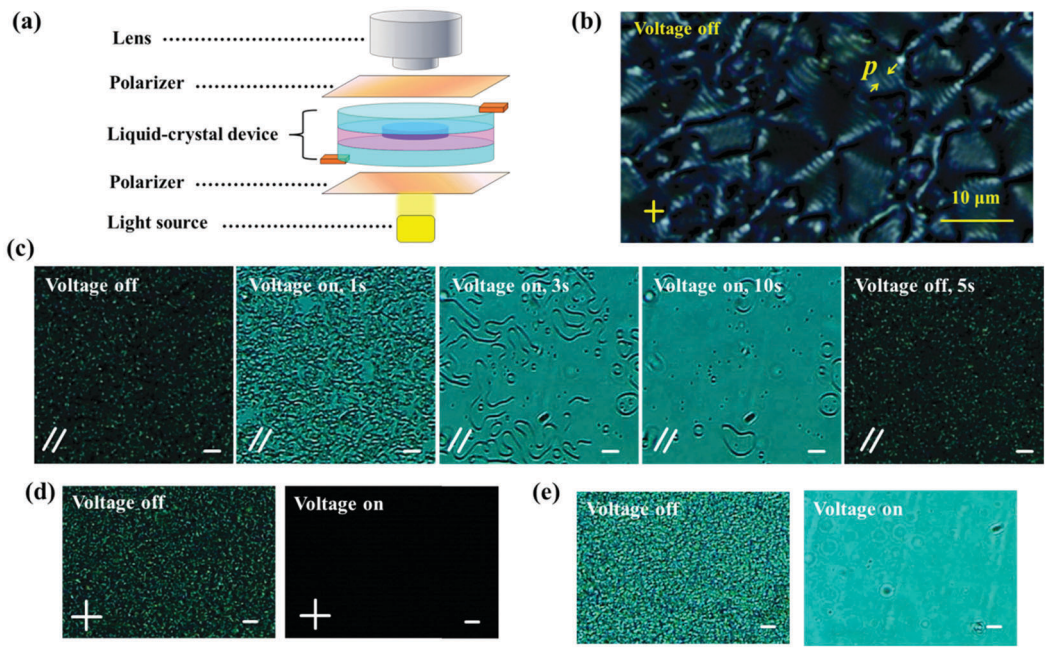

Fig. 3 Voltage-dependent microstructures. (a) Schematic of the experimental setup. (b) The focal conic texture of the cholesteric placed between perpendicular polarizers, observed at the voltage-off state. (c) Dynamic process of the cholesteric observed with parallel polarizers (Movie S2, ESI†) at a voltage of amplitude 500 V and frequency 1 kHz. (d) Device placed between perpendicular polarizers, observed at the voltage-off and voltage-on states (Movie S3, ESI†). (e) Device placed under the microscope without an analyzer, observed at the voltage-off and voltage-on states (Movie S4, ESI†). Scales bars in (c)–(e) indicate 100 μm.

conductors have similar electrooptical characteristics as those using electronic conductors.

The response time of the device is not limited by the resistivity of the hydrogels. The capacitors due to the dielectric elastomers, the liquid crystals and the EDLs are in series. The equivalent capacitance is dominated by the small capacitors of the dielectric and the liquid crystals, both of which are on the order of 10^{-10} F; while the large capacitance due to the EDLs, which are on the order of 10^{-5} F, is negligible. The resulting capacitance of the device C is $\sim 10^{-10}$ F. The resistance due to the hydrogel is $R_{gel} \sim 10^2\ \Omega$. As a result, the RC delay of the device is small, $\tau_{RC} \sim 10^{-8}$ s, and will not contribute to the observed switching time of the device.

We confirm the change of the cholesteric texture as a function of voltage under a microscope with one linear polarizer placed before the device, and with or without an analyzer after the device (Fig. 3a). In the absence of voltage, the cholesteric forms a focal conic texture, showing a pitch of ~ 2 μm (Fig. 3b). After the voltage is applied, the cholesteric domains unwind to align with the electric field. Homeotropic regions nucleate and grow with time. The remaining twisted domains form loops and threads; they decrease in length and gradually disappear. When the voltage is switched off, the twisted domains re-form. The dynamic process is observed when the device is placed between two parallel polarizers (Fig. 3c and Movie S2, ESI†). When the voltage is off, rotating the analyzer to be perpendicular to the polarizer (Fig. 3d) or removing the analyzer (Fig. 3e) does not affect the low intensity in the view, indicating a strong scattering of light by the focal conic domains. When the voltage is on, the device shows a homogeneous black field of view with the analyzer in perpendicular orientation (Fig. 3d and Movie S3, ESI†) or a homogeneous bright field of view without the analyzer (Fig. 3e and Movie S4, ESI†), indicating that the homeotropic liquid-crystal molecules do not scatter or modulate the polarized light.

We next demonstrate a stretchable electrooptical device (Fig. 4 and Fig. S3, ESI†). We apply a pre-stretch of ~ 1.3 to the VHB before fabricating the device, and regard this as the reference state. In the reference state, the thickness of the

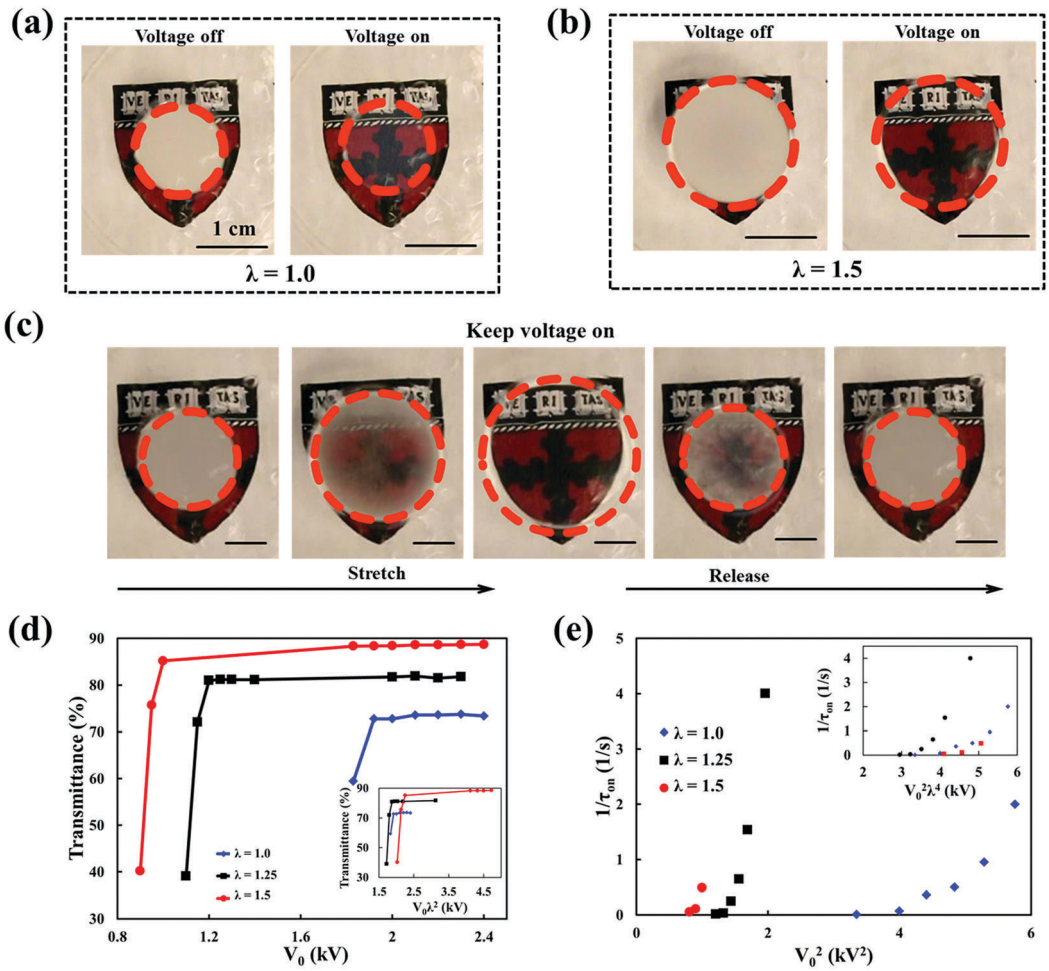

Fig. 4 Stretchable liquid-crystal device. (a) The device is switched in the undeformed state, $\lambda = 1.0$. (b) The device is switched in the stretched state, $\lambda = 1.5$. The dashed circles indicate the area containing the cholesteric. (c) The transparency changes in a cycle of stretching and releasing. A square-wave voltage of amplitude 1200 V and frequency 1 kHz is applied during the whole process. (d) The transmittance as a function of voltage at several values of stretch. The maximum transmittance increases while the threshold voltage for switching decreases as λ increases. Inset: The transmittance as a function of electric field intensity. (e) $1/\tau_{on}$, as a function of voltage squared at various λ. Inset: $1/\tau_{on}$ as a function of electric field squared.

cholesteric is $d \approx 296$ μm. Let λ be the stretch (*i.e.*, the diameter of the device in the stretched state divided by that in the reference state). The device remains switchable at both the reference state $\lambda = 1.0$ (Fig. 4a) and in the stretched state $\lambda = 1.5$ (Fig. 4b).

We also note a new mode of operation: the light shutter is switchable in response to a combined electrical voltage and mechanical force (Fig. 4c). When the device in the reference state is subject to a voltage of 1200 V, the active area remains opaque. Then when the device is stretched to a large area, without changing the voltage, the active area becomes transparent (Movie S5, ESI†). Since the transmittance as a function of electric field is steep, such an electromechanical light shutter switches-on and switches-off at a narrow range of voltage and stretching. When the device is pulled by an equal-biaxial stretch λ, the thickness of the device reduces by a factor of λ^2, and the switching voltage is also reduced by a factor of about λ^2 (Fig. 4d). The inset shows that the relation between the transmittance and the product $V_0\lambda^2$ remains nearly the same for different values of λ.

The small difference between the three curves in the inset of Fig. 4d is probably due to the elastic deflection of the dielectric and the hydrodynamic flow of the cholesteric, driven by the Maxwell stress (Fig. S4 and Movie S6, ESI†). This elastohydrodynamic–electrooptical coupling can be minimized by reducing the radius of the dielectric cell. The elastohydrodynamic–electrooptical coupling can, of course, enable devices of new functions, but we will not pursue this possibility here.

When the device is stretched, the same applied voltage can switch the device much faster. Since thinning of the cholesteric increases the electric field by a factor of λ^2, we expect $1/\tau_{on}$ to increase by a factor of ${V_0}^2\lambda^4$. In the experiments, τ_{on} does show a significant decrease as V_0 or λ increases (Fig. 4e), although $1/\tau_{on}$ does not strictly follow a linear relationship with ${V_0}^2\lambda^4$ (Fig. 4e, inset), especially when the voltage is higher or the stretch is larger. The deviation is also likely caused by the elastohydrodynamic effect.

The dielectric layers serve two functions. First, the dielectric layers prevent the mixing of the gel and the liquid crystal. Second, the dielectric layers prevent electrical breakdown even if the Maxwell stress causes the top and bottom surfaces to deflect into contact. The voltage in our experiment is high, but can be reduced by reducing the thickness of the dielectric and liquid crystal layers. One may even remove the dielectric and allow the liquid crystal to be in direct contact with the gels, as long as the gels and the liquid crystal are immiscible. The Maxwell stress will deflect the gels negligibly if the device is sandwiched between elastomers of suitable stiffness.

Lithium chloride also serves two functions. First, lithium chloride provides mobile ions after dissolving in water. Second, lithium chloride is a potent humectant. Whereas a hydrogel containing sodium chloride hydrogel dries out easily, the hydrogel containing 8.0 M lithium chloride can retain water at a relative humidity as low as 11%.[32] The device maintains its switching performance well even after being exposed to the open air for more than six months. For critical conditions such as a vacuum environment and temperatures below the freezing point or boiling point of the hydrogel, one can of course use ionogels instead.

Conclusions

We have used ionic conductors to realize organic liquid-crystal devices (OLCDs). Liquid crystals are anisotropic dielectrics. Their electrooptical effects require application of voltage, not injection of electrons. Consequently, ionic conductors can be used to drive liquid crystal devices of all kinds. The basic structure of the devices is compatible with surface patterning, distribution of particles, polymer-dispersed liquid crystals, and polymer-stabilized liquid crystals. Ionic conductors can also drive arrays of pixels. OLCDs are fully organic, and amenable to roll-to-roll and digital manufacturing.

The use of ionic conductors greatly expands the choice of transparent conductors. This large pool of materials will enable liquid-crystal devices of new characteristics. For example, one may choose a gel, an elastomer, and a liquid crystal to match their refractive indices, and thereby minimize the Fresnel reflections. In contrast, conventional liquid-crystal devices have mismatched reflective indices ($\sim$2.0 for ITO, and $\sim$1.5 for glass).

The new attribute of OLCDs—softness—may bring liquid crystals to new domains of applications, such as wearable displays for camouflage, and curved, deformable displays for entertainment. One can also imagine programmable, high-resolution, tissue-attachable patterns of light for optogenetics and optoceuticals—that is, a direct TV for the brain, heart, and skin.

Experimental section

Synthesis of the ionic conductor

The ionic conductor used in our experiment was a polyacrylamide hydrogel containing lithium chloride. To prepare the ionic conductor, we dissolved 2.4888 g of acrylamide (0.035 mol) and 5.94 g of lithium chloride (0.14 mol) in 17.5112 g of deionized water (0.973 mol). The resulting concentration of lithium chloride was 8.0 M. We then added 0.0015 g of the crosslinker (*N*,*N*′-methylenebisacrylamide, MBAA, 10^{-5} mol), 8 μL of the accelerator (*N*,*N*,*N*′,*N*′-tetramethylethylenediamine, TEMED, 5.3×10^{-5} mol), and 0.0025 g of the initiator (ammonium persulphate, APS, 1.1×10^{-5} mol) to the solution. After careful stirring, we transferred the solution into a glass mold with a 1 mm thick spacer, and placed the solution in a fume hood to cure at room temperature for 6 hours. The as-prepared ionic conductor was removed from the mold, cut into a pre-designed shape and then transferred onto the target device.

Preparation of the cholesteric liquid crystal

We made a cholesteric liquid crystal by mixing a nematic liquid crystal (4-cyano-4′-pentylbiphenyl, 5CB) and a chiral liquid crystal (4-(hexyloxy)-, 4-[[[(1r)-1-methylheptyl]oxy]carbonyl], R-811) at a

weight ratio of 95 : 5. The solution was homogenized using a vortex mixer (Digital Vortex Mixer, VWR) for 10 min.

Fabrication of electrooptical devices (Fig. S5, ESI†)

A layer of dielectric elastomer (VHB 4905, 3M) was cut into a disk with a hole at the center using a laser cutter (UNIVERSAL), followed by laminating onto another layer of VHB 4905. The two layers were fastened on a biaxial stretcher, pre-stretched and then mounted on a rigid circular-ring frame. The cholesteric liquid crystal was added into the hole. Another layer of VHB 4905 with the same pre-stretch was laminated to seal the liquid crystal, forming a liquid-crystal cell. The polyacrylamide hydrogel was cut into a circular shape with a tail for electrical connection, and then laminated on the two sides of the liquid-crystal cell. Two aluminum foils were placed on the hydrogels outside the active area to connect the device to the voltage source.

Electrooptical measurements

A signal generator (KEYSIGHT, 33500B) was used to supply square-wave signal at 1 kHz. The signal from the generator was fed through an amplifier (TRek, MODEL 30/20A) with a magnifying factor of 3000 to the two aluminum foils on the electro-optical device. The resulting voltage waveform had minimum and maximum amplitudes of $-V_0$ and $+V_0$, respectively, where V_0 was the set voltage. Optical transmittance was measured by placing the device between two collimating lenses, connected using optical fibers to a tungsten light source and a spectrometer (Ocean Optics, USB 2000+). Before the measurement, a voltage was applied for 5 s and removed to obtain an initial opaque state. Data were collected using a custom-made LabVIEW program.

Microscopic observation (Fig. S6, ESI†)

The device was observed under a microscope (Leica, DM 4000M) with one linear polarizer placed before the device, and with or without an analyzer after the device in either perpendicular or parallel orientation. A mobile phone was mounted on the ocular to record the dynamic process of the liquid-crystal device.

Conflicts of interest

There are no conflicts to declare.

Acknowledgements

The work is supported by NSF MRSEC (DMR 14-20570) and NSF CMMI-1404653. C. H. Yang was supported by the China Scholarship Council as a visiting scholar at Harvard University.

References

1 D.-K. Yang and S.-T. Wu, *Fundamentals of Liquid Crystal Devices*, John Wiley & Sons, Chichester, England, 2006.
2 R. Oldenbourg, *Polarization Microscopy with the LC-Polscope*, Cold Spring Harbor Laboratory Press, Cold Spring Harbor, 2005.
3 P. F. McManamon, J. Shi and P. J. Bos, *Opt. Eng.*, 2005, **44**, 128004.
4 O. Pishnyak, S. Sato and O. D. Lavrentovich, *Appl. Opt.*, 2006, **45**, 4576.
5 S. Susumu, S. Akira and S. Rumiko, *Jpn. J. Appl. Phys.*, 1985, **24**, L626.
6 S.-Y. Lu and L.-C. Chien, *Opt. Lett.*, 2010, **35**, 562.
7 V. Borshch, S. V. Shiyanovskii and O. D. Lavrentovich, *Phys. Rev. Lett.*, 2013, **111**, 107802.
8 P. A. Levermore, R. Jin, X. Wang, L. Chen, D. D. C. Bradley and J. C. de Mello, *J. Mater. Chem.*, 2008, **18**, 4414.
9 J. Huang, X. Wang, A. J. deMello, J. C. de Mello and D. D. C. Bradley, *J. Mater. Chem.*, 2007, **17**, 1043.
10 S.-I. Na, S.-S. Kim, J. Jo and D.-Y. Kim, *Adv. Mater.*, 2008, **20**, 4061.
11 Z. Chen, J. W. F. To, C. Wang, Z. Lu, N. Liu, A. Chortos, L. Pan, F. Wei, Y. Cui and Z. Bao, *Adv. Energy Mater.*, 2014, **4**, 1400207.
12 D. Chen, J. Liang and Q. Pei, *Sci. China: Chem.*, 2016, **59**, 659.
13 D. McCoul, W. Hu, M. Cao, V. Mehta and Q. Pei, *Adv. Electron. Mater.*, 2016, **2**, 1500407.
14 K. S. Kim, Y. Zhao, H. Jang, S. Y. Lee, J. M. Kim, K. S. Kim, J.-H. Ahn, P. Kim, J.-Y. Choi and B. H. Hong, *Nature*, 2009, **457**, 706.
15 G. Eda and M. Chhowalla, *Adv. Mater.*, 2010, **22**, 505.
16 P. H. Wöbkenberg, G. Eda, D.-S. Leem, J. C. de Mello, D. D. C. Bradley, M. Chhowalla and T. D. Anthopoulos, *Adv. Mater.*, 2011, **23**, 1558.
17 S. Yodyingyong, Q. Zhang, K. Park, C. S. Dandeneau, X. Zhou, D. Triampo and G. Cao, *Appl. Phys. Lett.*, 2010, **96**, 073115.
18 P. Blake, P. D. Brimicombe, R. R. Nair, T. J. Booth, D. Jiang, F. Schedin, L. A. Ponomarenko, S. V. Morozov, H. F. Gleeson, E. W. Hill, A. K. Geim and K. S. Novoselov, *Nano Lett.*, 2008, **8**, 1704.
19 J. Liang, L. Li, X. Niu, Z. Yu and Q. Pei, *Nat. Photonics*, 2013, **7**, 817.
20 S. Shian and D. R. Clarke, *Opt. Lett.*, 2016, **41**, 1289.
21 G. P. Crawford, *Flexible Flat Panel Displays*, John Wiley & Sons, Chichester, England, 2005.
22 J. Lewis, *Mater. Today*, 2006, **9**, 38.
23 K. Alzoubi, M. M. Hamasha, S. Lu and B. Sammakia, *J. Disp. Technol.*, 2011, **7**, 593.
24 S. P. Lacour, S. Wagner, Z. Huang and Z. Suo, *Appl. Phys. Lett.*, 2003, **82**, 2404.
25 D. J. Lipomi, M. Vosgueritchian, B. C.-K. Tee, S. L. Hellstrom, J. A. Lee, C. H. Fox and Z. Bao, *Nat. Nanotechnol.*, 2011, **6**, 788.
26 M. L. Hammock, A. Chortos, B. C. K. Tee, J. B. H. Tok and Z. Bao, *Adv. Mater.*, 2013, **25**, 5997.
27 S. Yang, E. Ng and N. Lu, *Extreme Mechanics Letters*, 2015, **2**, 37.

28 S. Yao and Y. Zhu, *Adv. Mater.*, 2015, **27**, 1480.
29 F. C. Krebs, *Org. Electron.*, 2009, **10**, 1636.
30 R. Søndergaard, M. Hosel, D. Angmo, T. T. Larson-Olsen and F. C. Krebs, *Mater. Today*, 2012, **15**, 36.
31 C. Keplinger, J. Y. Sun, C. C. Foo, P. Rothemund, G. M. Whitesides and Z. Suo, *Science*, 2013, **341**, 984.
32 Y. Bai, B. Chen, F. Xiang, J. Zhou, H. Wang and Z. Suo, *Appl. Phys. Lett.*, 2014, 151903.
33 A. K. Denisin and B. L. Pruitt, *ACS Appl. Mater. Interfaces*, 2016, **8**, 21893.
34 P. Lin, T. Zhang, X. Wang, B. Yu and F. Zhou, *Small*, 2016, **12**, 4386.
35 B. Chen, J. J. Lu, C. H. Yang, J. H. Yang, J. Zhou, Y. M. Chen and Z. Suo, *ACS Appl. Mater. Interfaces*, 2014, **6**, 7840.
36 J. Tang, J. Li, J. J. Vlassak and Z. Suo, *Extreme Mechanics Lett.*, 2017, **10**, 24.
37 R. Bai, Q. Yang, J. Tang, X. P. Morelle, J. J. Vlassak and Z. Suo, *Extreme Mechanics Letters*, 2017, **15**, 91.
38 A. Southan, M. Mateescu, V. Hagel, M. Bach, C. Schuh, C. Kleinhans, P. J. Kluger, S. Tussetschlager, I. Nuss, T. Haraszti, S. V. Wegner, J. P. Spatz, H. Boehm, S. Laschat and G. E. M. Tovar, *Macromol. Chem. Phys.*, 2013, **214**, 1865.
39 V. Hagel, M. Mateescu, A. Southan, S. V. Wegner, I. Nuss, T. Haraszti, C. Kleinhans, C. Schuh, J. P. Spatz, P. J. Kluger, M. Bach, S. Tussetschlager, G. E. M. Tovar, S. Laschat and H. Boehm, *Sci. Rep.*, 2013, **3**, 2043.
40 M. Martini, P. S. Hegger, N. Schadel, B. B. Minsky, M. Kirchhof, S. Scholl, A. Southan, G. E. M. Tovar, H. Boehm and S. Laschat, *Materials*, 2016, **9**, 810.
41 J. P. Gong, Y. Katsuyama, T. Kurokawa and Y. Osada, *Adv. Mater.*, 2003, **15**, 1155.
42 J. Y. Sun, X. Zhao, W. R. K. Illeperuma, O. Chaudhuri, K. H. Oh, D. J. Mooney, J. J. Vlassak and Z. Suo, *Nature*, 2012, **489**, 133.
43 J. Y. Sun, C. Keplinger, G. M. Whitesides and Z. Suo, *Adv. Mater.*, 2014, **26**, 7608.
44 H. Yuk, T. Zhang, G. A. Parada, X. Liu and X. Zhao, *Nat. Commun.*, 2016, **7**, 12028.
45 J. Le Bideau, L. Viau and A. Vioux, *Chem. Soc. Rev.*, 2011, **40**, 907.
46 R. L. Kerr, J. P. Edwards, S. C. Jones, B. J. Elliott and D. L. Gin, *Polym. J.*, 2016, **48**, 635.
47 C. H. Yang, B. Chen, J. J. Lu, J. H. Yang, J. Zhou, Y. M. Chen and Z. Suo, *Extreme Mechanics Letters*, 2015, **3**, 59.
48 C. Larson, B. Peele, S. Li, S. Robinson, M. Totaro, L. Beccai, B. Mazzolai and R. Shepherd, *Science*, 2016, **351**, 1071.
49 C. H. Yang, B. Chen, J. Zhou, Y. M. Chen and Z. Suo, *Adv. Mater.*, 2016, **28**, 4480.
50 S. S. Robinson, K. W. O'Brien, H. Zhao, B. N. Peele, C. M. Larson, B. C. M. Murray, I. M. V. Meerbeek, S. N. Dunham and R. F. Shepherd, *Extreme Mechanics Letters*, 2015, **5**, 47.
51 P. Manandhar, P. D. Calvert and J. R. Buck, *IEEE Sens. J.*, 2012, **12**, 2052.
52 J. Guo, X. Liu, N. Jiang, A. K. Yetisen, H. Yuk, C. Yang, A. Khademhosseini, X. Zhao and S.-H. Yun, *Adv. Mater.*, 2016, **28**, 10244.
53 C. C. Kim, H. H. Lee, K. H. Oh and J. Y. Sun, *Science*, 2016, **353**, 682.
54 J. Wang, C. Yan, G. Cai, M. Cui, A. L. S. Eh and P. S. Lee, *Adv. Mater.*, 2016, **28**, 4490.
55 K. H. Lee, M. S. Kang, S. Zhang, Y. Gu, T. P. Lodge and C. D. Frisbie, *Adv. Mater.*, 2012, **24**, 4457.
56 B. Chen, Y. Bai, F. Xiang, J. Y. Sun, Y. M. Chen, H. Wang, J. Zhou and Z. Suo, *J. Polym. Sci., Part B: Polym. Phys.*, 2014, **52**, 1055.
57 M. Kleman and O. D. Lavrentovich, *Soft Matter Physics: An Introduction*, Springer, New York, 2003.
58 R. B. Meyer, *Appl. Phys. Lett.*, 1968, **12**, 281.
59 J. J. Wysocki, J. Adams and W. Haas, *Phys. Rev. Lett.*, 1968, **20**, 1024.
60 A. J. Bard and L. R. Faulkner, *Electrochemical Methods: Fundamentals and Applications*, John Wiley & Sons, New York, 2000.
61 P. G. de Gennes and J. Prost, *The Physics of Liquid Crystals*, Clarendon Press, Oxford, 1993.